Oliveira, L. M. R.; Cardoso, A. J. M. and Cruz, S. M. A.: "Transformers on-load exciting current Park's Vector Approach as a tool for winding faults diagnostics", Conference Record of the 15th International Conference on Electrical Machines (ICEM 2002), CD-ROM, 6 pp., Brugge, Belgium, August 25-28, 2002.

Transformers On-Load Exciting Current Park's Vector Approach as a Tool for Winding Faults Diagnostics

Luís M. R. Oliveira[1,2], A. J. Marques Cardoso[1] and Sérgio M. A. Cruz[1]

[1] Universidade de Coimbra, Departamento de Engenharia Electrotécnica e de Computadores
Pólo II - Pinhal de Marrocos, P – 3030-290 Coimbra, Portugal
phone: +351 239 796232 – fax: +351 239 796247 – e-mail: ajmcardoso@ieee.org

[2] Escola Superior de Tecnologia da Universidade do Algarve
Campus da Penha, P – 8000-117 Faro, Portugal
e-mail: lolivei@ualg.pt

Abstract – **This paper presents the development of a new approach for diagnosing the occurrence of inter-turn short-circuits in the windings of three-phase transformers, which is based on the on-line monitoring of the on-load exciting current Park's Vector patterns. Experimental and simulated results demonstrate the effectiveness of the proposed technique for detecting winding inter-turn insulation faults in operating three-phase transformers.**

1. Introduction

Power and distribution transformers have formed an essential part of electricity supply networks since the alternating current system was adopted more than a century ago [1].

Under the deregulation policy of electric systems, each utility is trying to cut its costs, and the prevention of accidental loss is much more important than before. The capital loss of an accidental power transformer outage is often counted in million dollars for output loss only, not to say the costs associated with repair or replacement. Because of this economic incentive, preventive test and on-line monitoring are benefit to predict incipient fault conditions, and to schedule outage, maintenance and retirement of the transformers [2].

Therefore it is quite obvious the need for the development of on-line diagnostic techniques that would aid in transformers maintenance. A survey of the most important methods, actually in use, for condition monitoring and diagnostics of power and distribution transformers, presented in [3], stresses the need for the development of new diagnostic techniques, which can be applied without taking transformers out of service, and which can also provide a fault severity criteria, in particular for determining transformers winding insulation faults.

The most difficult transformer winding fault for which to provide protection is the fault that initially involves only one turn [4]. Initially, the insulation breakdown leads to internal arcing, which results into a low current, high impedance fault [5]. Usually, this incipient inter-turn insulation failure does not draw sufficient current from the line to operate an ordinary overload circuit-breaker or even more sensitive balanced protective gear [6]. This turn-to-turn fault will then progress, with random propagation speed, involving additional turns and layers, leading to a high current, low impedance fault, [7], [8]. The transformer will, in fact, be disconnected from the line automatically when the fault has extended to such degree as to embrace a considerable portion of the affected winding [6].

Previous research, concerning the use of the Park's Vector Approach, has demonstrated the effectiveness of this non-invasive technique for diagnosing malfunctions in operating three-phase induction motors, power electronics and adjustable speed drives [9]. Preliminary experimental results, presented in [3], concerning the use of the supply current Park's Vector Approach, have also demonstrated the effectiveness of this technique for diagnosing the occurrence of inter-turn insulation faults in the windings of operating three-phase transformers. The on-line diagnosis is based on identifying the appearance of an elliptic pattern, corresponding to the transformer supply current Park's Vector representation, whose ellipticity increases with the severity of the fault and whose major axis orientation is associated to the faulty phase. However, with this approach, it is difficult to discriminate between unbalanced loads and winding faults. To overcome this difficulty, an improved diagnostic technique was implemented, which consists in the analysis of the on-load exciting current Park's Vector pattern, and therefore unaffected by the transformer's load conditions.

The experimental study of winding inter-turn short-circuits occurrence presents some difficulties, mainly due to the high magnitudes of the faulty currents involved, which can damage the test transformer. Therefore, a detailed analysis of these phenomena can be better investigated by the use of a suitable digital simulation transformer model. For that purpose, a coupled electromagnetic transformer model was developed [10]-[12], which is based on the combination of both magnetic and electric lumped-parameters equivalent circuits, allowing for the modelling and simulation of the transformer in its natural technology.

With the aid of this transformer model, the on-load exciting current Park's Vector Approach will be applied for diagnosing the occurrence of winding insulation faults, which is the scope of this paper.

2. Digital Simulation of Winding Inter-Turn Short-Circuits

For winding fault studies, an open-structure transformer model is necessary, i.e., a model in which it would be possible to manipulate the windings arrangement. The coupled electromagnetic model, allowing for the modelling and simulation of the transformer in its natural technology, so that the cause-and-effect relationships can be closely investigated [13], becomes the natural choice for the analysis of transformer internal faults [11].

The coupled electromagnetic transformer model consists in the combination of both magnetic and electrical equivalent circuits (Fig. 1 and Fig. 2, respectively), in order to obtain the flux-current relationships:

$$\boldsymbol{\lambda} = \boldsymbol{L} \cdot \boldsymbol{i} \tag{1}$$

$$d\boldsymbol{\lambda}/dt = \boldsymbol{v} - \boldsymbol{R} \cdot \boldsymbol{i} \tag{2}$$

The faults are introduced in the model by dividing the affected winding in two parts, one corresponding to the healthy section and the other to the faulty subwinding, as shown in the equivalent circuits of Fig. 3. If the fault occurs in the primary winding, the short-circuited turns act as an autotransformer load on the winding, as shown in Fig. 3(a). However, if the fault takes place on the secondary winding, the short-circuited turns act as an ordinary double winding load, Fig. 3(b) [6].

The pertinent fault equivalent circuit is then introduced in the magnetic equivalent circuit (leading to one additional magnetomotive force in the faulty phase, Fig. 4) and in the electric equivalent circuit (leading to other several changes, Fig. 5). A detailed description of the model implementation is given in [10]-[12].

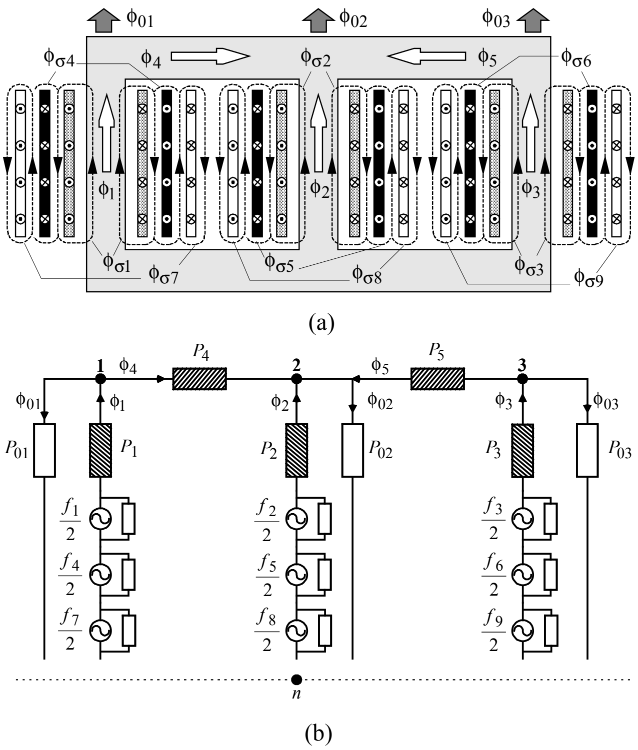

Fig. 1: (a) Flux distribution in a three-phase, three-limb, three-winding, core-type transformer, assuming a slightly greater magnetomotive force in the inner windings; (b) equivalent magnetic circuit.

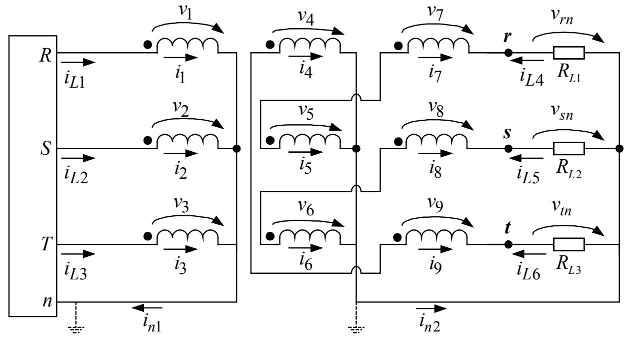

Fig. 2: Simplified equivalent electric circuit for the case of an *Ynzn5* connection and a balanced resistive load.

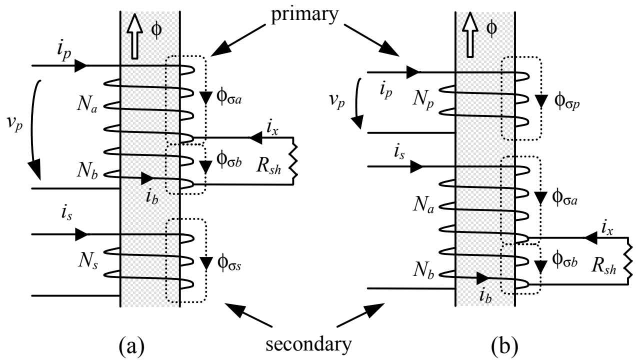

Fig. 3: Equivalent circuits for a fault occurring in the: (a) primary winding; (b) secondary winding.

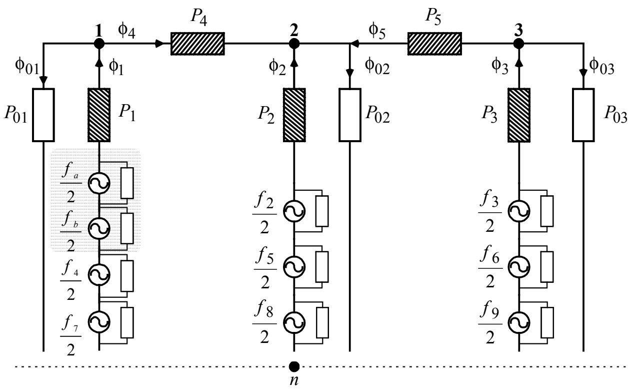

Fig. 4: Equivalent magnetic circuit for the case of a primary-side faulty winding (phase *R*).

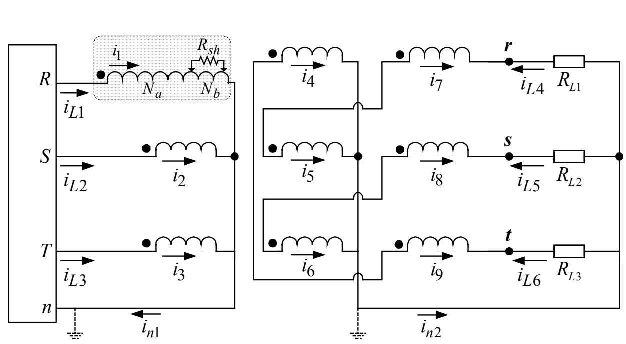

Fig. 5: Equivalent electric circuit for the case of a primary-side faulty winding (phase *R*).

3. Winding Faults Diagnostics

For the experimental investigation (and digital model validation), a three-phase, three-leg transformer, of 6 kVA, 220/127 V, was used. The transformer has four windings per limb, having two of them been modified by the addition of a number of tappings connected to the coils, allowing for the introduction of different percentages of shorted turns at several locations in the winding, as shown in Fig. 6 for the phase *R* of the transformer primary winding.

A shorting resistor (R_{sh}, in Fig. 3) was connected at the terminals of the faulty subwinding, whose value was chosen so as to create an effect strong enough to be easily visualised, but simultaneously big enough to limit the short-circuit current and thus protecting the test transformer from complete failure when the short is introduced.

A. Supply Current Park's Vector Approach

As a function of mains phase variables (i_R, i_S, i_T) the transformer current Park's Vector components (i_D, i_Q) are:

$$i_D = \left(\sqrt{2}/\sqrt{3}\right) i_R - \left(1/\sqrt{6}\right) i_S - \left(1/\sqrt{6}\right) i_T \tag{3}$$

$$i_Q = \left(1/\sqrt{2}\right) i_S - \left(1/\sqrt{2}\right) i_T \tag{4}$$

Under ideal conditions, the three-phase currents lead to a Park's Vector with the following components:

$$i_D = \left(\sqrt{6}/2\right) i_M \sin(\omega t) \tag{5}$$

$$i_Q = \left(\sqrt{6}/2\right) i_M \sin(\omega t - \pi/2) \tag{6}$$

where:

i_M maximum value of the supply current (A);

ω angular supply frequency (rad/s);

t time variable (s).

The corresponding representation is a circular locus centered at the origin of the coordinates. Under abnormal conditions equations (5) and (6) are no longer valid and consequently the observed picture differs from the reference pattern. The operating philosophy of the Park's Vector Approach is thus based on identifying unique signature patterns in the figures obtained, corresponding to the transformer current Park's Vector representation.

For the case of the *Ynzn*5 connection, a balanced resistor load and 10% of permanent shorted turns in the phase *R* of the transformer primary winding, both experimental and simulated primary-side phase currents waveforms are shown in Fig 7(a) and 7(b), respectively, which are in relatively good agreement.

The occurrence of primary-side inter-turn short-circuits leads to an increment in the magnitude of the current in the affected winding, as compared to a healthy condition, which results in an unbalanced system of primary currents. For this reason, the magnitude of the primary neutral current (i_{n1}=i_{L1}+i_{L2}+i_{L3}), is also affected.

For the same aforementioned conditions, the experimental and simulated fault related currents waveforms are shown in Fig. 8(a) and 8(b). The faulty subwinding current, i_b, is approximately in phase opposition with i_1 (*Lenz* law). The current in the short-circuit auxiliary resistor, i_x, has a higher magnitude than i_b, since $i_x = i_b - i_1$ (notation as per Fig. 3(a), and, in this case, $i_p = i_1$).

In the presence of the primary winding inter-turn short-circuits, the secondary-side currents do not present any relevant change as compared to the transformer's healthy operation, remaining an approximately balanced three-phase system.

For the same load conditions and transformer winding connections mentioned above, Fig. 9 presents the experimental primary-side phase current Park's Vector patterns, for several percentages of shorted turns in the primary windings and for different faulty phases. The primary-side phase current Park's Vector pattern, corresponding to the healthy operation, differs slightly

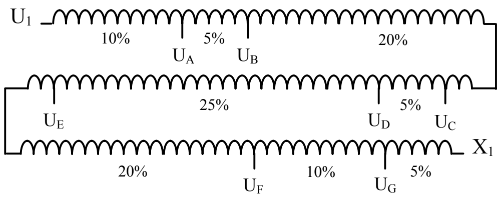

Fig. 6: Location of the tappings for transformer primary winding (phase *R*).

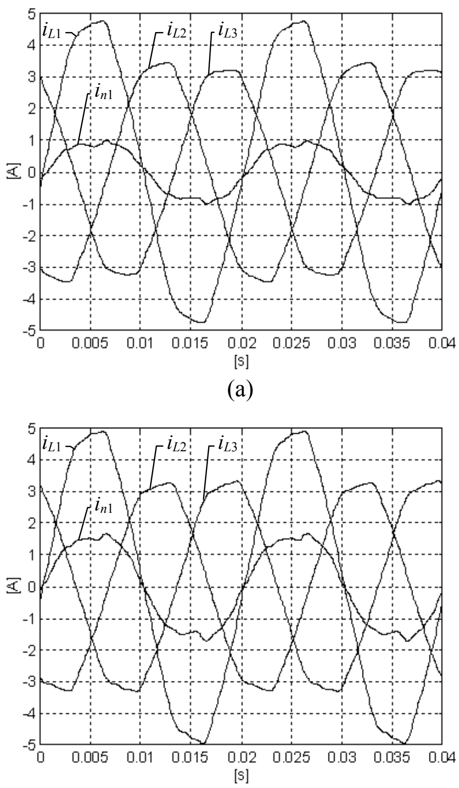

(a) (b)

Fig. 7: Supply currents waveforms for the case of a *Ynzn*5 connection, a resistive balanced load and 10% of shorted turns (permanent) in the primary winding (phase *R*): (a) experimental; (b) simulated.

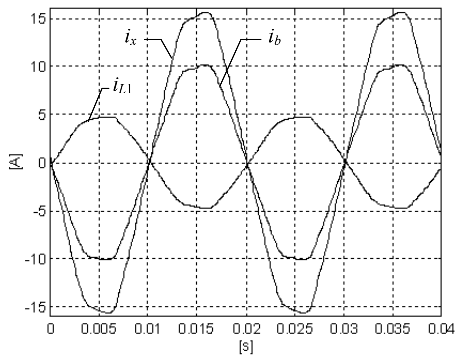

(a)

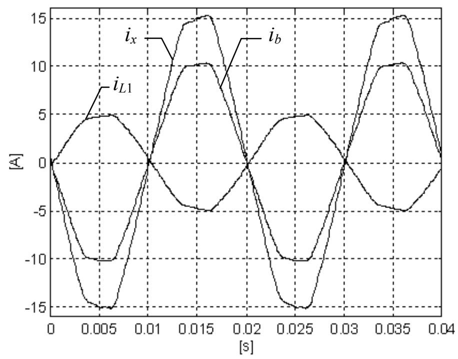

(b)

Fig. 8: Fault related currents waveforms for the case of a *Ynzn*5 connection, a resistive balanced load and 10% of shorted turns (permanent) in the primary winding (phase *R*): (a) experimental; (b) simulated.

from the circular locus expected for ideal conditions, due to, among others, the supply voltage harmonic content and the minor reluctance seen from the central limb, with respect to the lateral limbs [3].

The occurrence of primary-side inter-turn short-circuits manifests itself in the deformation of the primary-side phase current Park's Vector pattern corresponding to a healthy condition, leading to an elliptic representation, whose ellipticity increases with the severity of the fault and whose major axis orientation is associated to the faulty phase. Similar conclusions, concerning the transformer supply current Park's Vector patterns, can be drawn for the occurrence of secondary inter-turn short circuits, under the same load conditions and winding connections [3].

The simulated primary-side supply current Park's Vector patterns are presented in Fig. 10, which are in close agreement with the experimental results of Fig. 9.

The transformer secondary current Park's Vector pattern doesn't provide any indication about inter-turn short--circuits that may occur, either in the primary or in the secondary side of the transformer. However, it plays a very important role for discriminating the presence of unbalanced loads.

Consider, for example, the case of an unbalanced load with $R_{L2}=R_{L3}=R_{L1}/5$ and, simultaneously, 10% of shorted turns in the primary winding of phase *R*. From the resultant primary-side current Park's Vector pattern, shown in Fig. 11(a), it is difficult to detect the fault, being necessary to make use of the secondary-side current Park's Vector

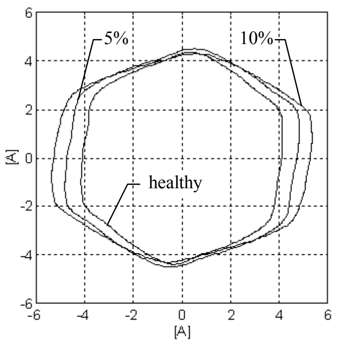

(a)

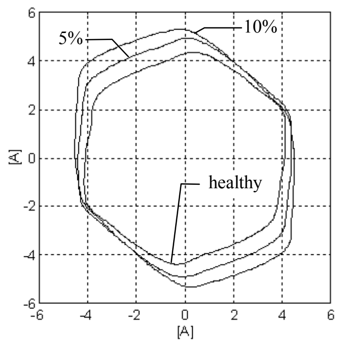

(b)

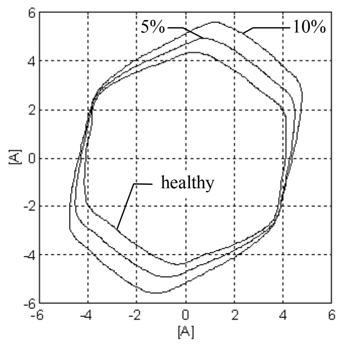

(c)

Fig. 9: Experimental primary-side phase current Park's Vector patterns for the case of a *Ynzn*5 connection and a balanced resistive load, with several percentages of permanent shorted turns in the primary windings and for different faulty phases: (a) phase *R*; (b) phase *S*; (c) phase *T*.

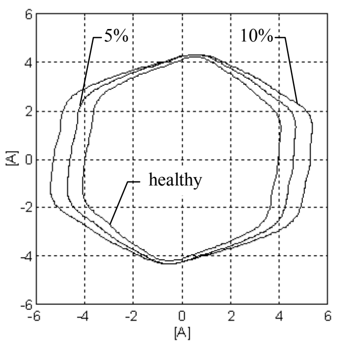

(a)

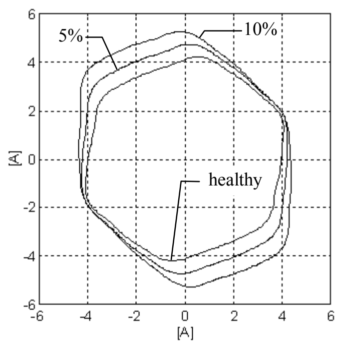

(b)

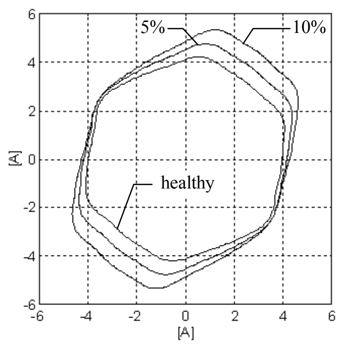

(c)

Fig. 10: Simulated primary-side phase current Park's Vector patterns for the case of a *Ynzn*5 connection and a balanced resistive load, with several percentages of permanent shorted turns in the primary windings and for different faulty phases: (a) phase *R*; (b) phase *S*; (c) phase *T*.

pattern to recognize the unbalanced load condition of the transformer. Consequently, with this diagnostic technique, it is difficult to discriminate between unbalanced loads and winding faults.

B. On-Load Exciting Current Park's Vector Approach

To overcome the above-mentioned difficulty, an improved diagnostic technique was implemented, which consists in the analysis of the on-load exciting current Park's Vector pattern, and therefore unaffected by the transformer's load conditions. The on-load exciting currents are computed by adding the magnetomotive forces along each limb of the transformer, resulting, for the *Ynzn*5 connection (notation as per Fig. 2):

$$\begin{bmatrix} i_{exc1} \\ i_{exc2} \\ i_{exc3} \end{bmatrix} = \begin{bmatrix} i_{L1} \\ i_{L2} \\ i_{L3} \end{bmatrix} + \frac{N_2}{N_1} \begin{bmatrix} -1 & 0 & 1 \\ 1 & -1 & 0 \\ 0 & 1 & -1 \end{bmatrix} \cdot \begin{bmatrix} i_{L4} \\ i_{L5} \\ i_{L6} \end{bmatrix} \qquad (7)$$

With this approach the on-line characteristic of the formerly diagnostic technique is maintained.

For the same case presented above, the resultant on-load exciting current Park's Vector pattern can be seen in Fig. 11(b), from which the fault is clearly detected. The same operating philosophy of the supply current Park's Vector Approach can again be applied to identify the severity and the phase location of the fault. Additionally, the on-load exciting current Park's Vector Approach enhances the severity of the fault, as compared to the former diagnostic technique, as shown in Figs. 12 and 13.

For the case of an incipient fault, involving only two shorted turns (≈1%), the supply current Park's Vector pattern does not provide any indication about the inter-turn short-circuit (Fig. 14(a)), whereas the analysis of the on-

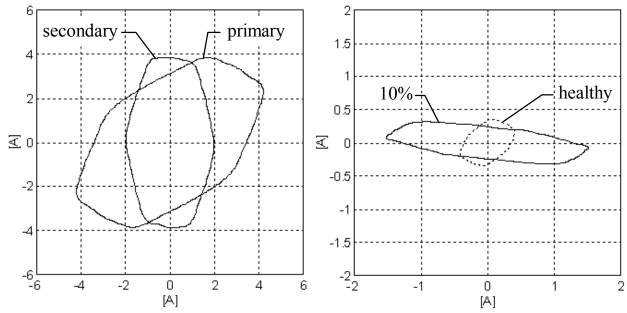

(a) (b)

Fig. 11: Simulated primary and secondary winding currents Park's Vector patterns (a) and on-load exciting current Park's Vector patterns (b), for the case of a *Ynzn*5 connection, an unbalanced resistive load and 10% of shorted turns in the primary winding (phase *R*).

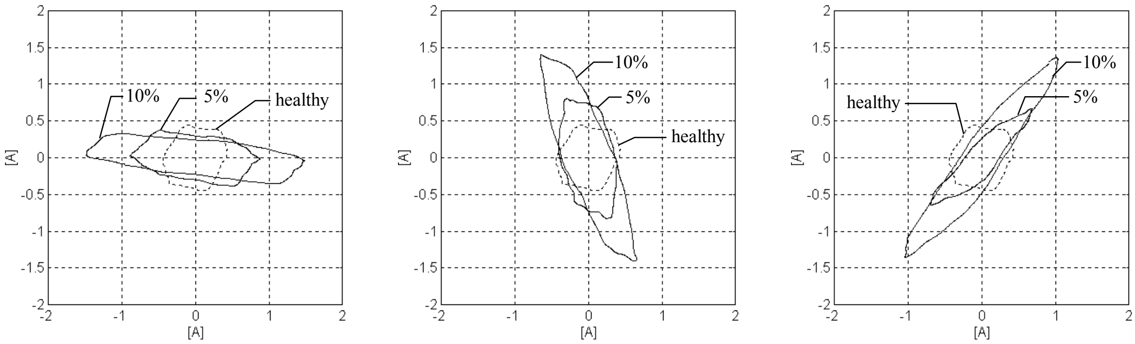

(a) (b) (c)

Fig. 12: Experimental on-load exciting current Park's Vector patterns for the case of a *Ynzn*5 connection and a balanced resistive load, with several percentages of permanent shorted turns in the primary windings and for different faulty phases: (a) phase *R*; (b) phase *S*; (c) phase *T*.

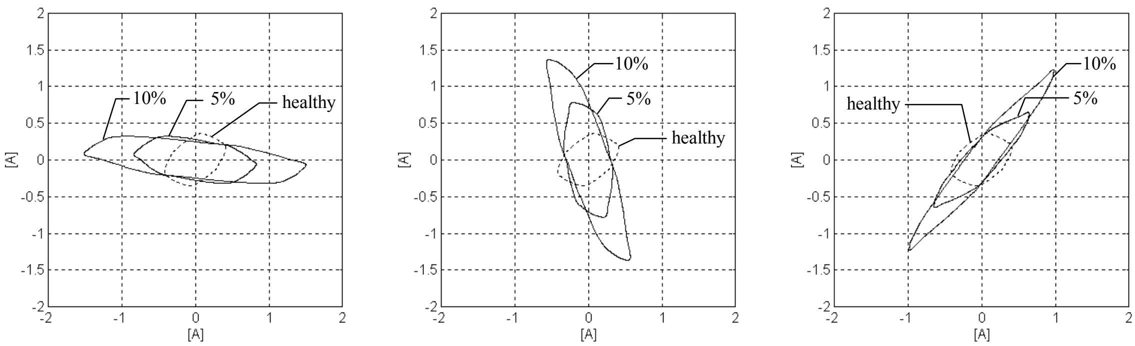

(a) (b) (c)

Fig. 13: Simulated on-load exciting current Park's Vector patterns for the case of a *Ynzn*5 connection and a balanced resistive load, with several percentages of permanent shorted turns in the primary windings and for different faulty phases: (a) phase *R*; (b) phase *S*; (c) phase *T*.

-load exciting current Park's Vector Approach clearly reveals the presence of the fault, Fig. 14(b). Other experimental and simulated tests carried out for different types of the transformer windings connection lead to similar conclusions to the ones presented before [12], [14]. Additionally, it has been demonstrated that the detection of intermittent winding faults is also possible [15].

4. Conclusions

This paper presents the development of a new approach for diagnosing the occurrence of inter-turn short-circuits in the windings of operating three-phase transformers, which consists in the analysis of the on-load exciting current Park's Vector patterns. The on-line diagnosis is based on identifying the appearance of an elliptic pattern, corresponding to the transformer on-load exciting current Park's Vector representation, whose ellipticity increases with the severity of the fault and whose major axis orientation is associated to the faulty phase. Additionally, a digital coupled electromagnetic transformer model is presented for winding faults studies.

Experimental and/or simulated test results were presented, which demonstrate the effectiveness of the diagnostic technique.

Further work is currently in progress, concerning the refinement of the proposed diagnostic technique, with the aim of dealing with the simultaneous occurrence of winding faults, unbalanced supply voltages, unbalanced loads, or even the surrounding presence of power electronics equipment.

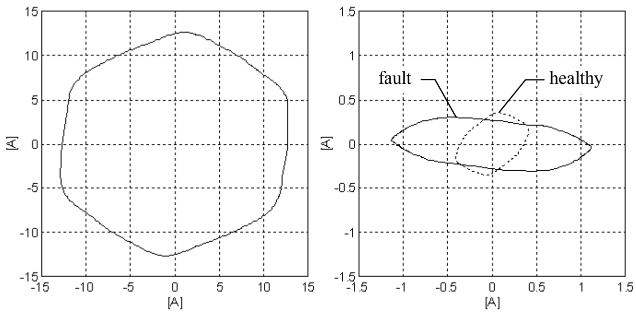

(a) (b)

Fig. 14: Simulated supply current Park's Vector pattern (a) and on-load exciting current Park's Vector pattern (b), for the case of a *Ynzn*5 connection, a balanced resistive load and two shorted turns (≈1%) in the primary winding (phase *R*).

Acknowledgement

The authors wish to acknowledge the financial support of the Portuguese Foundation for Science and Technology, under Project Number POSI/EEI/14151/1998.

References

[1] C. Ashmore, "Transforming technology," *International Power Generation*, Vol. 22, No. 3, pp. 25-26, March 1999.

[2] Z. Wang, "Artificial intelligence applications in the diagnosis of power transformer incipient faults," Ph. D. thesis, Faculty of the Virginia Polytechnic Institute and State University, 2000.

[3] A. J. M. Cardoso and L. M. R. Oliveira, "Condition monitoring and diagnostics of power transformers," *International Journal of COMADEM*, Vol. 2, No. 3, pp. 5-11, July 1999.

[4] IEEE Std. C37.91-2000, "IEEE guide for protective relay applications to power transformers," IEEE 2000.

[5] P. Barkan, B. L. Damsky, L. F. Ettlinger, and E. J. Kotski, "Overpressure phenomena in distribution transformers with low impedance faults: experiment and theory," *IEEE Transactions on Power Apparatus and Systems*, Vol. 95, No. 1, pp. 37-48, January/February 1976.

[6] S. A. Stigant and A. C. Franklin, The J&P Transformer Book, 10th Edition, Newnes-Butterworths, London (1973).

[7] C. W. Plummer, G. L. Goedde, E. L. Petit, J. S. Godbee and M. G. Hennessey, "Reduction in distribution transformer failures rates and nuisance outages using improved lightning protection concepts," *IEEE Transactions on Power Delivery*, Vol. 10, No. 2, pp. 768-777, April 1995.

[8] J. M. Lunsford and T. J. Tobin, "Detection of and protection for internal low-current winding faults in overhead distribution transformers," *IEEE Transactions on Power Delivery*, Vol. 12, No. 3, pp. 1241-1249, July 1997.

[9] A. J. M. Cardoso, "The Park's Vector Approach: a general tool for diagnostics of electrical machines, power electronics and adjustable speed drives," in *Record of the 1997 IEEE International Symposium on Diagnostics for Electrical Machines, Power Electronics and Drives*, pp. 261-269.

[10] L. M. R. Oliveira and A. J. M. Cardoso, "Three-phase, three-limb, steady-state transformer model: the case of a *Ynzn* connection," in *Proceedings of the IASTED International Conference, "Power and Energy Systems"*, pp. 467-472, 2000.

[11] L. M. R. Oliveira and A. J. M. Cardoso, "A coupled electromagnetic transformer model for the analysis of winding inter-turn short-circuits," in *Record of the IEEE International Symposium on Diagnostics for Electrical Machines, Power Electronics and Drives*, pp. 367-372, 2001.

[12] L. M. R. Oliveira, "Development and implementation of a digital model for transformer winding fault studies – An introduction to a new diagnostic method," (in Portuguese), M.Sc. thesis, University of Coimbra, Portugal, 2001.

[13] R. Yakamini and H. Bronzeado, "Transformer inrush calculations using a coupled electromagnetic model," *IEE Proc. Sci. Meas. Technol.*, Vol. 141, No. 6, pp. 491-498, November 1994.

[14] L. M. R. Oliveira and A. J. M. Cardoso, "Fault diagnostics of operating three-phase transformers by the on-load exciting current Park's Vector Approach," (in Portuguese), in *7th National Maintenance Congress*, pp. 853-866, 2002.

[15] L. M. R. Oliveira and A. J. M. Cardoso, "On-line diagnostics of transformer winding insulation failures, by Park's Vector Approach," to be presented at the *9th International Electrical Insulation Conference – INSUCON 2002*.